MORPHOMETRIC COMPARISON OF MARTIAN IRON METEORITE FINDS WITH CURATED TERRESTRIAL ANALOG SAMPLES USING 3D VISUALIZATION AND MEASUREMENT TECHNIQUES. J. W. Ashley[1], A. G. Curtis[1], S. J. Oij[1], D. F. Wellington[2], and P. –Y. Meslin[3], [1]Jet Propulsion Laboratory, California Institute of Technology, Pasadena, CA 91109; james.w.ashley@jpl.nasa.gov, [2]School of Earth and Space Exploration, Arizona State University, Tempe, AZ 85287, [3]L'Institut de Recherche en Astrophysique et Planétologie, 31400 Toulouse, France.

Introduction: Since the identification of Heat Shield Rock at Meridiani Planum as a IAB complex iron-nickel meteorite by Opportunity in 2005 [1], nearly 40 additional rocks of probable exogenic origin (most of them iron-nickel) have been found at the Gusev crater, Meridiani Planum and Gale crater rover landing sites. Some of these have been found in recent sols and a considerable body of compositional information has been collected with interesting results [see 2; this conference]. With each new meteorite find, the relevance of exogenic materials to Mars science has been enhanced. The science topics approachable through the study of these rocks are many and diverse, often complimenting science conducted using indigenous materials: Some address environments in which the meteorites are found (physical and chemical weathering processes, prevailing wind directions through geologic time, etc.) [3-6]. Others address atmospheric density at the time of fall [7]. Still others use meteoritic iron and dust for the study of thermal emission behavior on Mars [8]. One analysis uses relative timing of nearby crater ejecta blanket emplacement to help estimate the first quantitative weathering rate for Amazonian Mars [9]. Speculation that chondritic materials could both preserve biosignatures and encourage the colonization of indigenous bacteria on Mars is also in discussion [10].

We focus here on iron meteorite surface morphologies to help resolve Amazonian weathering processes (and their relative timing) responsible for modifying a suite of surfaces with unique malleabilities and reactivities across three widely separated landing sites along equatorial martian latitudes.

Post-fall Surface Modification: Thus meteorites found on Mars provide complementary insights into chemical and physical surface alteration processes. The effects of weather reflect these processes and associated exposure histories, and include acidic corrosion, aeolian scouring and oxide production on Mars. The challenge is to identify and separate features resulting from ablataion (produced during atmospheric passage) from weathering (produced post-fall). Ablation features speak to the freshness of the sample, and include regmaglypts, pits, grooving, and fusion crusts.

The swell and swail, thumprint-shaped features common to fresh iron meteorite falls on Earth are known as regmaglypts. They are caused by supersonic buffeting during atmospheric entry and are indications of unmodified surfaces [11]. Portions of the martian iron suite of meteorites share the appearance of regmaglypts, and this has been used in qualitative discussions to infer relative degrees of surface modification. However because of the similarity in appearance of some ablation features to those produced by aeolian scouring, this hypothesis must be tested using measurements of suspected regmaglypts and associated ablation features in comparison to those of curated terrestrial analog samples.

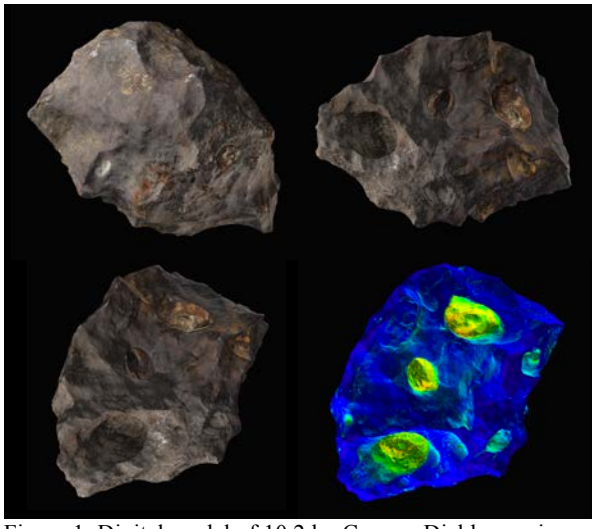

Figure 1. Digital model of 10.2 kg Canyon Diablo specimen. Our lighting/imaging technique penetrates weathered troilite nodule recesses (yellow-green) to include entire inner surface areas.

Methods: Because of the high density of iron meteorites, three-dimensional visualization of large irons offers many obvious advantages for morphological assessment: The ability to quickly orient, directly measure and compare features, and screen for surface patterns is greatly enhanced by this capability. The first step in this process lies in producing the data products. Several iron meteorites (Sikhote-Alin, Canyon Diablo, and Bruno) were examined and imaged using standard SLR camera equipment at the Center for Meteorite Studies (CMS) at Arizona State University. Visualization models were created at JPL using multiview photogrammetry (Structure from Motion). Masking to remove non-meteorite sections of the images was key to successful 3D reconstruction. Placing meteorites on a white turntable inside a shadow-free lightbox (AmazonBasics Protable Photo Studio) great-

ly reduced the effort required for image masking. Agisoft Meshlab and Blender 3D graphic software are used for reconstruction, UV-unwrapping, and visual rendering.

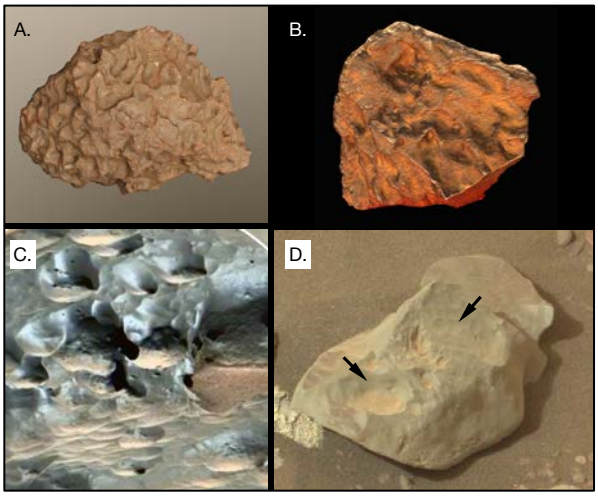

Figure 2. A) 3D visualization model of Sikhote Alin shows classic terrestrial regmaglypt forms. B) The 12.7 kg iron meteorite Bruno exhibits classic regmaglypt and associated flow structures with striated fusion crust. C) ChemCam RMI image mosaic of Lebanon A meteorite (Curiosity sol 640). Note highly variable, superposing, and undercutting character of scallop and hollow forms, some of which may be original regmaglypts, while others are likely post-fall modifications. Image credit: NASA/JPL/LANL. D) Right Mastcam frame of iron-nickel meteorite candidate Rockend (Curiosity sol 2173). Long axis is approximately 7 cm. Note variable scale for scallop features (arrows) across the rock surface. NASA/JPL/Mastcam.

Micro-Digital Elevation Model (MicroDEM) creation using MER Microscopic Imager (MI) stereo pairs is also being performed for the Block Island and Shelter Island meteorites to assess surface topography on a sub-millimeter scale. Since the MI camera is monoscopic, the MicroDEM is generated using simulated stereo by taking two images of a target, one with the camera shifted to a slight horizontal offset. With stereo imaging, the location of each pixel in 3D space can be found. The 3D data is then projected onto a defined vector, representing the normal of a surface plane. The projected data makes up the MicroDEM, displaying the height of each pixel relative to the defined surface plane.

Preliminary results: Our visualization techniques have produced 3D models that exceed anticipated results. Morphometric comparisons of martian irons with these 3D vizualization models using a variety of model measurement techniques are in progress. Metrics for quantifying the morphometric features of meteorite surfaces include the centerpoint to centerpoint spatial distribution of hollows to address the troilite acidification hypothesis outlined in [6,11]; and depth, diameter, and orientation geometry of scallops, flutes and regmaglypts to address ablation-related surface morphologies relevant to post-fall modification severity (important for establishing weathering rate/fall timing relationships), and possible paleowind direction imprints.

Because high-resolution images are used to blanket the point cloud surfaces, the models can be used for intimate visual study in concert with the topographic data (typically of coarser fidelity within the model). Massive iron meteorites weighing many tens of kilograms can be re-oriented easily for direct measurement of any surface feature (Figures 1,2). Topographic information penetrates to regions deep within recesses due to lighting geometry used at the time of imaging (Figure 1). MicroDEMs permit sub-millimeter measurements of surface topography useful for confirming the relative timing of coating emplacement, Widmanstätten structures, and suspected ablation features (Figure 3).

Ablation feature morphologies on terrestrial irons can vary depending on size, orientation during fall and fall velocity/duration [11]. However, our preliminary results suggest that these features can be quantified and distinguished from those produced post-fall as environmental modifications.

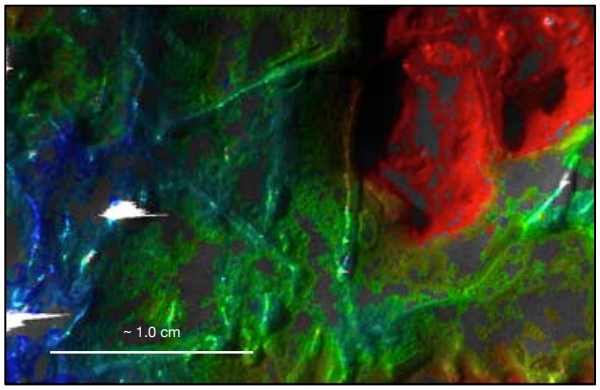

Figure 3. MicroDEM (digital elevation model) using Microscopic Imager stereo pair from the Block Island meteorite. Red zones show depth within possible regmaglypt structures. NASA/JPL/MI/MIPL:1M302456886EFFA5B8P2956M2M1.VIC and 1M302456978EFFA5B8P2936M2M1.VIC.

References: [1] Connolly H. C. J., et al. (2006) *Meteorit. Planet. Sci.* 41, 1383-1418. [2] Meslin P. –Y., et al. (2019); *this conference*. [3] Schröder C., et al. (2008) *J. Geophys. Res.* 113 E06S22. [4] Ashley J. W., et al. (2011) *JGR* 116, E00F09. [5] Ashley J. W. and Golombek M. P. (2016) *LPSC XLVII, abs. #*2461. [6] Fleischer I., et al. (2011) *MAPS,* 46, issue 1, 21-34. [7] Chappelow J. E. Golombek M. P. (2010) *J. Geophys. Res.* 113 E06S22. [8] Ashley J. W., et al. (2008) *LPSC XXXIX, abs. #*2382. [9] Schröder C., et al. (2016) *Nat Comm* 7, 13459. [10] Tait A. W., et al. (2019) *this conference.* [11] Buchwald (1975) Handbook of Iron Meteorites, 1418 pp., *Univ. of Calif. Press.*